PHYSICAL REVIEW A VOLUME 9, NUMBER 5 MAY 1974

Photoionization from excited states of helium

V. L. Jacobs*
Theoretical Studies Group (Code 602), Goddard Space Flight Center, National Aeronautics and Space Administration, Greenbelt, Maryland 20771
(Received 9 November 1973)

The cross sections for photoionization from the $2\,^1S$, $2\,^3S$, $2\,^1P$, and $2\,^3P$ excited states of helium are calculated for photoelectron energies below the $n=2$ threshold of He^+ using Hylleraas bound-state wave functions and $1s2s2p$ close-coupling final-state wave functions. The resonant structures associated with the lowest-lying ^1S, ^1P, ^3P, and ^1D autoionizing states of helium are found to be characterized by large values of the line-profile parameter q. The cross sections and the photoelectron angular-distribution asymmetry parameters for the P states are calculated for various polarization states of the target atom and the incident photon. Experiments which would lead to the separate determinations of the S- and D-wave partial photoionization cross sections are discussed.

I. INTRODUCTION

Photoionization from excited states of helium plays an important role in the transfer of radiation through laboratory plasmas[1] and hot stellar atmospheres.[2] In addition, accurate cross sections for single- and multiphoton ionization from excited states of helium may be required for a quantitative understanding of the interaction of laser radiation with a helium discharge.[3] Recent advances in atomic-beam methods and in frequency-tunable laser techniques have led to an accurate experimental determination of the photoionization cross sections for the $2\,^1S$ and $2\,^3S$ metastable states of helium in the near-threshold region.[4] Accordingly, the theoretical investigation of photoionization processes from excited states of helium is worthwhile.

In this paper, the cross sections for single-photon ionization from the $2\,^1S$, $2\,^3S$, $2\,^1P$, and $2\,^3P$ states of helium are evaluated for photoelectron energies below the $n=2$ threshold of the residual He^+ ion, using $1s2s2p$ close-coupling final-state continuum wave functions. Results for the $2\,^1S$ cross section in the nonresonant region have been reported in two earlier papers[5,6] and the near-threshold values[6] are in good agreement with the experimental determination. More recent theoretical studies of photoionization from the $1\,^1S$, $2\,^1S$, and $2\,^3S$ states of helium were restricted to photoelectron energies above the $n=2$ threshold,[7-9] where transitions can occur to the $2s$ and $2p$ excited states of He^+, and the resulting photoelectron angular distribution is a function of energy. From these studies and from the results of a recent helium photoionization experiment,[10] it has become apparent that the inclusion of close coupling between degenerate excited states of the He^+ ion is essential, not only for the accurate calculation of the resonance properties below the excitation threshold,[11] but also for the correct determination of the distribution between the degenerate ionic states above the threshold.

Norcross[12] has evaluated the $2\,^1S$ and $2\,^3S$ helium photoionization cross sections using $1s2s2p$ close-coupling continuum wave functions, but he employed Hartree-Fock bound-state wave functions which are not expected to be as accurate as the Hylleraas wave functions used in the present calculation. In previous evaluations of the $2\,^1P$ and $2\,^3P$ helium photoionization cross sections, the final continuum states were represented by hydrogenic[13] and quantum defect[14,15] wave functions. These approximations may provide reliable estimates in the near-threshold region, but they cannot account for the prominent resonant features which are predicted by the $1s2s2p$ close-coupling calculations.

An important feature of photoionization from excited states of helium is the significant enhancement of the total cross sections which results from taking into account transitions to excited states of the He^+ ion. It is therefore not surprising that the resonant structure associated with the $n=2$ threshold has been found to be more conspicuous in the photoionization continua of the metastable states than in the ground-state continuum. This fact is clearly illustrated by the line-profile parameters reported by Norcross[12] for the lowest-six ^1P resonance in the $2\,^1S$ cross section, which are in some cases more than a hundred times larger than the corresponding parameters obtained for the helium ground state by Burke and McVicar.[11]

The study of photoionization processes from the $2\,^1P$ and $2\,^3P$ states of helium would be difficult with present experimental techniques because of

the short radiative lifetimes of these excited states in comparison with the helium metastable states. However, photoabsorption from the P states using laser light may ultimately provide the most precise method for the experimental investigation of the S- and D-wave ionization continua of the helium atom.

In contrast to photoionization from the helium S states, photoelectric transitions from the P states will in general give rise to an energy-dependent photoelectron angular distribution below the $n=2$ threshold. In the case of unpolarized P states the angular distribution can be characterized by a single asymmetry parameter β regardless of the polarization state of the incident radiation.[16-19] The angular distribution of photoelectrons from polarized P states can be determined from a knowledge of two asymmetry parameters, which may show a complicated dependence on the initial polarization states.

An important simplification would occur if the helium atom could first be excited into an aligned P state and then ionized by linearly or circularly polarized photons incident in a suitable direction with respect to the atomic quantization axis. In these cases, the D partial-wave ionization continuum will be observed directly, and the photoelectron angular distribution below the $n=2$ threshold will not depend on the incident-photon energy.

II. THEORY OF DIFFERENTIAL PHOTOIONIZATION CROSS SECTIONS

A formulation of the theory of differential cross sections for atomic photoelectric transitions has been developed in terms of the irreducible tensor components of the initial and final polarization states.[19] In this section it is appropriate to present the results of this formulation which are applicable when the ejected electron and the residual ion polarizations are not measured. The discussion will be further restricted to cases where the coordinate system can be chosen to reduce the form of the differential cross section (for the transition to the nl_1 state of He^+) to the Legendre polynomial expansion

$$\sigma_{nl_1}(\vec{k}_n)=\frac{\sigma_{nl_1}}{4\pi}\left(1+\sum_{L>0}\beta_{nl_1,L}\,P_L(\cos\theta)\right), \tag{1}$$

where the appropriate definition of θ will depend on the initial polarization states. It is important to note that the electric-dipole selection rules allow only a few even values of L to contribute.

The initial bound state of the helium atom may be specified by a principal quantum number n_0 and by the total orbital and spin angular momenta L_0 and S_0. The polarization state of the helium atom with respect to the orbital angular momentum L_0 may be represented by a $(2L_0+1)\times(2L_0+1)$ density matrix ρ_0, which can be expressed in terms of the complete set of $(2L_0+1)^2$ irreducible tensor operators[20] in the form of the multipole expansion

$$\langle ML_0|\,\rho_0\,|ML_0'\rangle=\sum_{K_0N_0}\rho_0(K_0,N_0)(-1)^{L_0-ML_0}\times(2K_0+1)^{1/2}\begin{pmatrix}L_0 & K_0 & L_0\\ -ML_0 & N_0 & ML_0'\end{pmatrix}. \tag{2}$$

Similarly, the polarization state of the incident electric-dipole photon may be represented by a 3×3 density matrix ρ_γ, which will depend on the orientation of the photon beam with respect to the atomic quantization axis. It will also be convenient to expand ρ_γ in the form (2) with irreducible tensor components denoted by $\rho_\gamma(K_\gamma,N_\gamma)$. Explicit expressions for the irreducible tensor components of the initial polarization states that are treated in this paper have been given previously.[19]

The final-state continuum channels of the He^+-e^- system are defined by the quantum numbers nl_1l_2, L_TS_0, where l_2 is the photoelectron relative orbital angular momentum and L_T is the total orbital angular momentum.

The expressions which are derived for the total cross section σ_{nl_1} (in units of a_0^2) and the asymmetry parameters $\beta_{nl_1,L}$ may be written in the forms

$$\sigma_{nl_1}=4\pi^2\alpha\omega\sum_{l_2L_T}\sum_{K}(-1)^{1+L_0+L_T}\begin{Bmatrix}L_0 & L_0 & K\\ 1 & 1 & L_T\end{Bmatrix}\rho_0(K,0)\rho_\gamma(K,0)|M(l_2,L_T)|^2 \tag{3}$$

and

$$\beta_{nl_1,L}=\frac{4\pi^2\alpha\omega}{\sigma_{nl_1}}\sum_{l_2,L_T}\sum_{l_2',L_T'}\sum_{K_0}\sum_{K_\gamma}(-1)^{l_1+L_T}(2L+1)[(2K_0+1)(2K_\gamma+1)(2l_2+1)(2l_2'+1)(2L_T+1)(2L_T'+1)]^{1/2}\times\begin{pmatrix}l_2 & l_2' & L\\ 0 & 0 & 0\end{pmatrix}\begin{pmatrix}K_0 & K_\gamma & L\\ 0 & 0 & 0\end{pmatrix}\begin{Bmatrix}l_2 & l_2' & L\\ L_T' & L_T & l_1\end{Bmatrix}\begin{Bmatrix}L_0 & 1 & L_T'\\ L_0 & 1 & L_T\\ K_0 & K_\gamma & L\end{Bmatrix}\rho_0(K_0,0)\rho_\gamma(K_\gamma,0)M(l_2,L_T)M(l_2',L_T')^*, \tag{4}$$

where ω is the incident-photon energy measured in rydbergs ($\omega = I_0 + k_1^2$, where I_0 is the ionization potential) and α is the fine-structure constant. The summations are to be taken over all values of the angular momenta which are consistent with the selection rules associated with the 3-j, 6-j, and 9-j symbols. The transition amplitudes $M(l_2, L_T)$ may be defined in terms of either the dipole length or the dipole velocity forms of the matrix elements as follows:

$$M^{(L)}(l_2, L_T) = e^{i(\sigma_{l_2} - l_2\pi/2)} \times (nl_1 l_2, L_T S_0 \| \vec{r}_1 + \vec{r}_2 \| n_0 L_0 S_0) , \quad (5)$$

$$M^{(V)}(l_2, L_T) = (2e^{i(\sigma_{l_2} - l_2\pi/2)}/\omega) \times (nl_1 l_2, L_T S_0 \| \vec{\nabla}_1 + \vec{\nabla}_2 \| n_0 L_0 S_0) , \quad (6)$$

where σ_{l_2} denotes the Coulomb phase shift for the He^+ ion. In the reduced matrix elements of the dipole operators the final continuum states are assumed to be normalized to a Dirac δ function in the photoelectron energy.

The theory presented up to this point can be applied to any helium transition and, in fact, to any atomic system for which the LS representation is appropriate. In the remainder of this paper only transitions to $He^+(1s)$ will be treated, and therefore, the subscripts nl_1 will be omitted.

The photoelectron angular distribution resulting from ionization of unpolarized helium atoms is given by Eq. (1) with only the $L = 2$ term included in the summation. The associated asymmetry parameter is customarily denoted by β. When the incident radiation is linearly polarized θ measures the angle between the photoelectron momentum $\vec{k}_1$ and the photon polarization direction. For unpolarized or circularly polarized photons it is necessary only to replace β by $-\beta/2$ and to define θ as the angle between the photoelectron and incident photon propagation directions. For photoionization from the helium S states, the well-known result that β is identically 2, independent of energy, can be recovered from Eqs. (3) and (4). In the case of unpolarized P states, the interference between the transition amplitudes corresponding to the S- and D-channels will result in an energy dependence of the asymmetry parameter β which is expected to be rapid in the vicinity of an autoionization feature.

The photoelectron angular distribution from aligned ($ML_0 = 1$) P states of helium is determined by a knowledge of two asymmetry parameters, corresponding to $L = 2$ and 4. In the cases of incident photons with linear polarization in the direction of the atomic quantization axis and unpolarized or right circularly polarized photons propagating along the atomic quantization axis, the definitions given previously for θ still apply. For the circular and linear polarizations, only the D partial-wave channel will be excited in the photoelectric transition and the asymmetry parameters β_2 and β_4 will then be independent of energy.

III. HELIUM WAVE FUNCTIONS

The 2^1S, 2^3S, 2^1P, and 2^3P bound excited states of the helium atom are represented with high precision by the Hylleraas wave functions

$$\Psi_{n_0 L_0 S_0}(\vec{r}_1, \vec{r}_2) = \left(\frac{1 + (-1)^{S_0} P_{12}}{\sqrt{2}}\right) e^{-ar_1 - br_2} \times \sum_{ijk} C_{ijk} r_1^i r_2^j r_{12}^k Y_{00}(\hat{r}_1) Y_{L_0 M L_0}(\hat{r}_2) , \quad (7)$$

where P_{12} is the electron exchange operator. The values for the exponential parameters a and b were taken from the work of Accad and co-workers,[21] and 56-term expansions were computed by diagonalizing the matrices of the Hamiltonian operator.

The ${}^1L_T$ and ${}^3L_T$ final-state continuum wave functions with $L_T = 0, 1, 2$ are expanded in the close-coupling form[22]

$$\Psi^{(-)}_{1S,\, l_2 = L_T,\, S}(\vec{r}_1, \vec{r}_2) = \left(\frac{1 + (-1)^S P_{12}}{\sqrt{2}}\right) \sum_{n' l_1' l_2'} \frac{P_{n' l_1'}(r_1)}{r_1} \frac{F^{(-)}_{n' l_1' l_2'}(r_2)}{r_2} \times \sum_{m_1' m_2'} \langle l_1' l_2', L_T M L_T | l_1' m_1', l_2' m_2' \rangle \, Y^{m_1'}_{l_1'}(\hat{r}_1) Y^{m_2'}_{l_2'}(\hat{r}_2) , \quad (8)$$

where $P_{n' l_1'}(r_1)$ is the reduced He^+ ion radial wave function. The incoming-wave boundary condition appropriate to the description of the photoionization process is indicated by the superscript (−).

The coupled integrodifferential equations which are satisfied by the ejected electron radial wave functions $F^{(-)}_{n' l_1' l_2'}(r_2)$ were solved in the $1s2s2p$ close-coupling approximation for the photoelectron energy range $0.15 \leq k_1^2 \leq 2.80$ using the collision code of Burke and McVicar.[11] The photoelectric

transition matrix elements were then evaluated from the numerical continuum wave functions and the bound-state weight functions as described previously.[5,11]

IV. PHOTOIONIZATION CROSS SECTIONS

The L_T-wave partial cross section for the photoelectric transition

$$\mathrm{He}(n_0L_0S_0)+\hbar\omega\rightarrow\mathrm{He}^+(1s)+e^-(l_2=L_T) \tag{9}$$

from an unpolarized L_0 state of helium, is conveniently expressed in terms of the oscillator strength per unit rydberg energy interval df_{L_T}/dE according to the relation

$$\sigma_{L_T}=4\pi^2\alpha\frac{df_{L_T}}{dE}\,. \tag{10}$$

The oscillator strength may be defined in terms of the transition amplitudes introduced in Sec. I by

$$\frac{df_{L_T}}{dE}=\frac{\omega}{3(2L_0+1)}\,|M(l_2=L_T,\,L_T)|^2. \tag{11}$$

It is important to note that the cross section σ_{L_T} given by Eq. (10) is independent of the photon polarization.

The oscillator strengths associated with the $2\,^1S\rightarrow E\,^1P$ and $2\,^3S\rightarrow E\,^3P$ transitions are presented for the photoelectron energy range $0.15\leq k_1^2\leq 2.4$ in Tables I and II, respectively. Because the evaluations of the two alternative forms of the transition matrix elements are known to depend most strongly on different regions of configuration space, the fact that in most cases the length and velocity results differ by only a few percent may be taken as an indication of their reliability. The present results are in good agreement with the oscillator strengths calculated by Norcross[12] in the near-threshold region, but at the higher energies there are differences of more than 10%. Since the same final-state wave functions have been employed in both calculations, the discrepancies must be attributed to inaccuracies in the

TABLE I. The oscillator strength for the $2\,^1S$ state of helium. The length and velocity results are denoted by L and V, respectively. The numbers in parentheses are the powers of ten by which the entries are to be multiplied.

k_1^2 (Ry)	$\left(\frac{df}{dE}\right)_L$	$\left(\frac{df}{dE}\right)_V$
0.15	0.5545	0.5903
0.20	0.4736	0.4805
0.25	0.4008	0.4022
0.30	0.3431	0.3402
0.40	0.2564	0.2519
0.60	0.1528	0.1503
0.80	0.9842 (−1)	0.9713 (−1)
1.00	0.6737 (−1)	0.6635 (−1)
1.20	0.4812 (−1)	0.4696 (−1)
1.40	0.3526 (−1)	0.3398 (−1)
1.60	0.2611 (−1)	0.2480 (−1)
1.80	0.1922 (−1)	0.1797 (−1)
2.00	0.1364 (−1)	0.1254 (−1)
2.20	0.8589 (−2)	0.7695 (−2)
2.40	0.2869 (−2)	0.2372 (−2)

TABLE II. The oscillator strength for the $2\,^3S$ state of helium. The length and velocity results are denoted by L and V, respectively. The numbers in parentheses are the powers of ten by which the entries are to be multiplied.

k_1^2 (Ry)	$\left(\frac{df}{dE}\right)_L$	$\left(\frac{df}{dE}\right)_V$
0.15	0.4385	0.4498
0.20	0.3914	0.4111
0.25	0.3466	0.3642
0.30	0.3074	0.3235
0.40	0.2442	0.2567
0.60	0.1625	0.1712
0.80	0.1148	0.1211
1.00	0.8491 (−1)	0.8960 (−1)
1.20	0.6527 (−1)	0.6882 (−1)
1.40	0.5183 (−1)	0.5460 (−1)
1.60	0.4244 (−1)	0.4464 (−1)
1.80	0.3588 (−1)	0.3766 (−1)
2.00	0.3164 (−1)	0.3311 (−1)
2.20	0.3038 (−1)	0.3162 (−1)
2.40	0.4648 (−1)	0.4768 (−1)

TABLE III. The S- and D-wave partial oscillator strengths for the $2\,^1P$ state of helium. The length and velocity results are denoted by L and V, respectively. The numbers in parentheses are the powers of ten by which the entries are to be multiplied.

k_1^2 (Ry)	$\left(\frac{df_S}{dE}\right)_L$	$\left(\frac{df_S}{dE}\right)_V$	$\left(\frac{df_D}{dE}\right)_L$	$\left(\frac{df_D}{dE}\right)_V$
0.15	0.3467 (−1)	0.3720 (−1)	0.3350	0.4201
0.20	0.2621 (−1)	0.2634 (−1)	0.2196	0.2211
0.25	0.2033 (−1)	0.2030 (−1)	0.1540	0.1527
0.30	0.1626 (−1)	0.1598 (−1)	0.1107	0.1081
0.40	0.1091 (−1)	0.1043 (−1)	0.6027 (−1)	0.5733 (−1)
0.60	0.5625 (−2)	0.5178 (−2)	0.2060 (−1)	0.1913 (−1)
0.80	0.3288 (−2)	0.2988 (−2)	0.7940 (−2)	0.7222 (−2)
1.00	0.2114 (−2)	0.1935 (−2)	0.3201 (−2)	0.2810 (−2)
1.20	0.1486 (−2)	0.1380 (−2)	0.1247 (−2)	0.1010 (−2)
1.40	0.1134 (−2)	0.1075 (−2)	0.3970 (−3)	0.2663 (−3)
1.60	0.9465 (−3)	0.9154 (−3)	0.5795 (−4)	0.1507 (−4)
1.80	0.8787 (−3)	0.8652 (−3)	0.1306 (−4)	0.5505 (−4)
2.00	0.9578 (−3)	0.9540 (−3)	0.2489 (−3)	0.3841 (−3)
2.20	0.1463 (−2)	0.1466 (−2)	0.1091 (−2)	0.1347 (−2)
2.40	0.1436 (−1)	0.1433 (−1)	0.5340 (−2)	0.5815 (−2)

TABLE IV. The S- and D-wave partial oscillator strengths for the $2\,^3P$ state of helium. The length and velocity results are denoted by L and V, respectively. The numbers in parentheses are the powers of ten by which the entries are to be multiplied.

k_1^2 (Ry)	$\left(\frac{df_S}{dE}\right)_L$	$\left(\frac{df_S}{dE}\right)_V$	$\left(\frac{df_D}{dE}\right)_L$	$\left(\frac{df_D}{dE}\right)_V$
0.15	0.4146 (−1)	0.4825 (−1)	0.4484	
0.20	0.3280 (−1)	0.3801 (−1)	0.3617	0.3715
0.25	0.2546 (−1)	0.2780 (−1)	0.2691	0.2664
0.30	0.2046 (−1)	0.2235 (−1)	0.2058	0.2013
0.40	0.1404 (−1)	0.1485 (−1)	0.1272	0.1223
0.60	0.7237 (−2)	0.7489 (−2)	0.5658 (−1)	0.5367 (−1)
0.80	0.4149 (−2)	0.4253 (−2)	0.2917 (−1)	0.2778 (−1)
1.00	0.2512 (−2)	0.2612 (−2)	0.1678 (−1)	0.1608 (−1)
1.20	0.1606 (−2)	0.1701 (−2)	0.1052 (−1)	0.1010 (−1)
1.40	0.1073 (−2)	0.1156 (−2)	0.7043 (−2)	0.6748 (−2)
1.60	0.7290 (−3)	0.8104 (−3)	0.4975 (−2)	0.4734 (−2)
1.80	0.5127 (−3)	0.5819 (−3)	0.3669 (−2)	0.3459 (−2)
2.00	0.3666 (−3)	0.4242 (−3)	0.2809 (−2)	0.2617 (−2)
2.20	0.2634 (−3)	0.3110 (−3)	0.2222 (−2)	0.2047 (−2)
2.40	0.1869 (−3)	0.2255 (−3)	0.1819 (−2)	0.1659 (−2)

bound-state wave functions used by Norcross.[12]

The S- and D-wave partial oscillator strengths df_S/dE and df_D/dE for photoionization from unpolarized $2\,^1P$ and $2\,^3P$ states of helium are tabulated for the energy range $0.15 \leq k_1^2 \leq 2.4$ in Tables III and IV, respectively. The total cross sections are obtained by adding the two partial-wave contributions. As anticipated the D partial-wave contribution is dominant near the threshold in both cases, and for the $2\,^3P$ state the dominance of the ^3D-wave partial cross section extends over the entire energy range considered. The increased importance of the $2\,^1P \rightarrow E\,^1S$ transition at higher energies is attributable mainly to the occurrence of a zero minimum in the ^1D cross section. The agreement between the length and velocity results is very good except at the zero minimum.

The total photoionization cross sections for the $2\,^1S$ and $2\,^3S$ states and for unpolarized $2\,^1P$ and $2\,^3P$ states of helium are shown in Fig. 1 for photoelectron energies in the nonresonant region below the $n=2$ threshold. The cross sections for photoionization from the P states, while decreasing more rapidly away from the first ionization threshold, are predicted to be comparable to the S state cross sections in the near-threshold region. In a previous calculation for the $1\,^1S$ and $2\,^1S$ cross sections,[6] the continuum asymptotic expansion developed by Norcross[12] was incorporated into the collision code of Burke and McVicar[11] so that it could be operated for $k_1^2 < 0.15$. This procedure was not set up for the present calculations. However, the cross sections exhibit an approximately linear threshold behavior as functions of wavelength. This suggests that an accurate extrapolation procedure should be possible.

The resonant features associated with the lowest ^1S, ^1P, ^1D, and ^3P helium autoionizing states are clearly visible in the semilogarithmic cross-section plots presented in Figs. 2 and 3. Each partial wave contribution was fitted to the Fano line-shape formula[23]

$$\frac{df_{L_T}}{dE} = \left(\frac{df_{L_T}}{dE}\right)_0 \frac{(\epsilon + q_{L_T})^2}{1+\epsilon^2}\,, \tag{12}$$

where ϵ is defined in terms of the resonance position E_r and the width Γ_r according to the relation

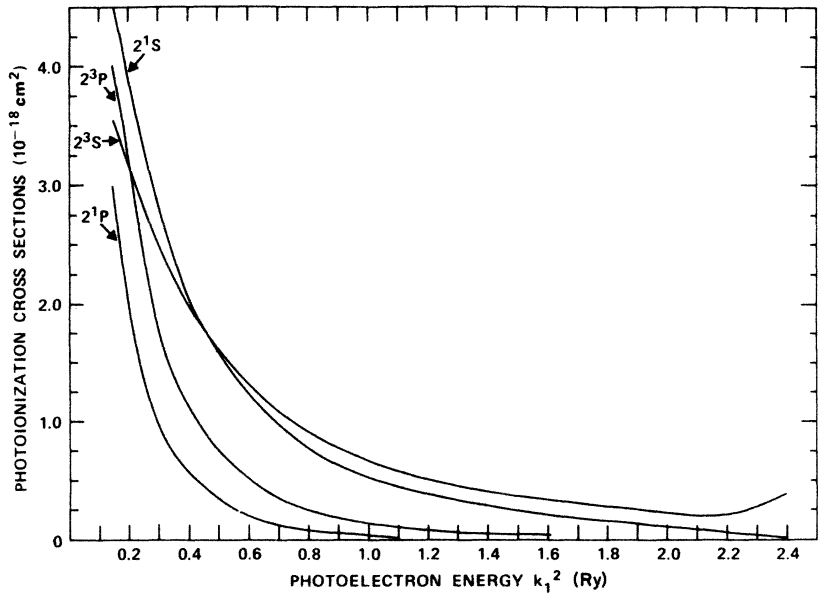

FIG. 1. The photoionization cross sections for the $2\,^1S$ and $2\,^3S$ states and for unpolarized $2\,^1P$ and $2\,^3P$ states of helium in the nonresonant region, evaluated using the length matrix elements.

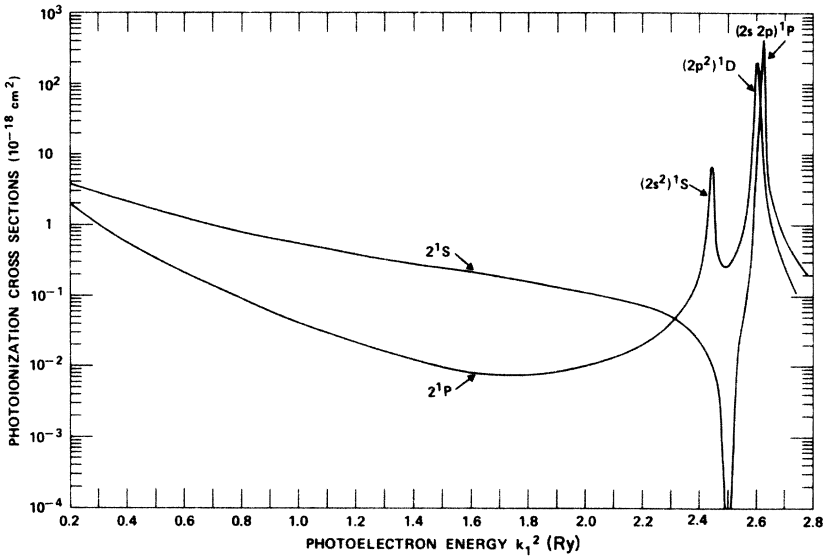

FIG. 2. Resonant features in the photoionization cross sections for the $2\,^1S$ state and for an unpolarized $2\,^1P$ state of helium.

$$\epsilon = 2(E - E_r)/\Gamma_r . \tag{13}$$

The positions and widths obtained for the resonances are identical to the values given by Burke and McVicar,[11] since the same computer program was used. The nonresonant background oscillator strength $(df_{L_T}/dE)_0$ was allowed to vary linearly with ϵ through the resonance. The line-profile parameter q_{L_T} and the background oscillator strength (evalulated at $\epsilon = 0$) which were obtained for each resonance are given in Table V.

The most important result of the analysis is that the resonant shapes considered are found to be characterized by large values of the line-profile parameter q_{L_T}, particularly for the last three transition in Table V. A significant enhancement of the photoionization cross sections for these three transitions might have been anticipated, since they involve single-electron excitations. From the result that the value of q_{L_T} is large it follows that the resonant profile described by Eq. (12) is more nearly Lorentzian and that the $\Delta E = \Gamma_r/2q_{L_T}$ displacement of the peak from the resonance position E_r is negligible.

The zero minimum in the ^1D-wave partial photoionization cross section appears to be the dip associated with the $(2p^2)\,^1D$ resonance, which is predicted by the analytic form (12) to occur at $\epsilon = -q_{L_T}$. The occurrence of the suppression of the D-wave photoionization continuum several

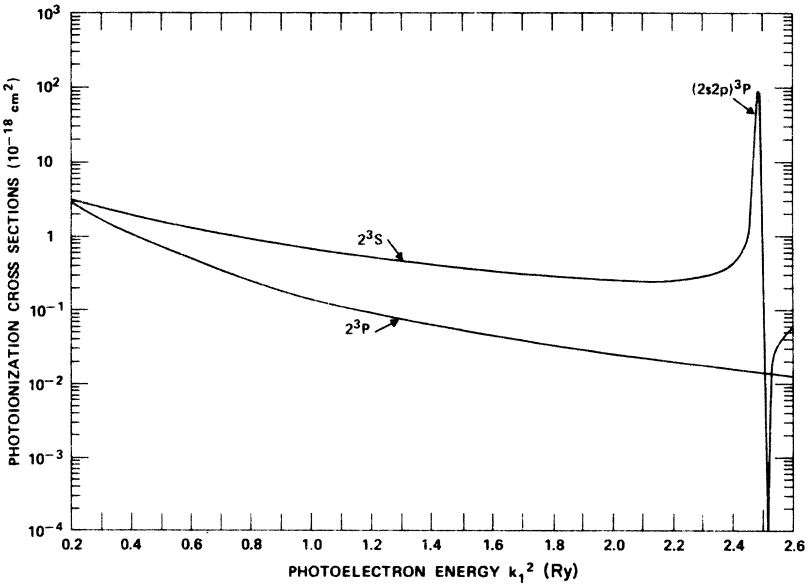

FIG. 3. The $(2s\,2p)\,^3P$ resonance in the $2\,^3S$ helium photoionization cross section and the photoionization cross section for an unpolarized $2\,^3P$ state of helium.

TABLE V. The line-profile parameter q_{L_T} and the background oscillator strength $(df_{L_T}/dE)_0$ obtained for the lowest-lying ^1S, ^3P, ^1P, and ^1D helium resonances using the length matrix elements. The numbers in parentheses are the powers of ten by which the entries are to be multiplied.

Transition	E_r(eV) [a]	Γ_r(eV) [a]	q_{L_T}	$\left(\frac{df_{L_T}}{dE}\right)_0$
$2\,^1P \rightarrow (2s^2)\,^1S$	57.865 [b]	1.41 (−1)	−29.30	9.487 (−4)
$2\,^3S \rightarrow (2s2p)\,^3P$	58.360	1.06 (−2)	−122.4	1.521 (−2)
			−106.6 [c]	2.17 (−2) [c]
$2\,^1P \rightarrow (2p^2)\,^1D$	60.025	7.32 (−2)	172.4	7.792 (−4)
$2\,^1S \rightarrow (2s2p)\,^1P$	60.269	4.38 (−2)	76.21	8.175 (−3)
			64.73 [c]	1.29 (−2) [c]

[a] Reference 11.
[b] E_r is measured with respect to the helium ground state.
[c] Reference 12.

times the width below the resonance position is, therefore, attributable to the large positive value of the line-profile parameter. In the case of the helium metastable states, Table V indicates some rather large discrepancies between the line-profile parameters and background oscillator strengths obtained from the present calculations and the values reported by Norcross.[12] These discrepancies may be accounted for by the assumption that q_{L_T} is energy-independent which, as has been pointed out by Norcross,[12] may not be valid for large values of q_{L_T}.

For a polarized L_0 state of the helium atom, the total photoionization cross section may still be expressed as an incoherent superposition of individual L_T wave contributions given by Eq. (10) provided the factor $1/3(2L_0+1)$ in the definition of the oscillator strength (11) is replaced by

$$(-1)^{i+L_0+L_T} \sum_K \rho_0(K,0)\rho_r(K,0) \begin{Bmatrix} L_0 & L_0 & K \\ 1 & 1 & L_T \end{Bmatrix} . \tag{14}$$

As an illustration of the effect of the atomic polarization for the case of unpolarized light, the photoionization cross sections for unpolarized and for aligned ($ML_0=1$) $2\,^1P$ and $2\,^3P$ states of helium are compared in Table VI.

In the case of photionization from aligned helium P states by right circularly (linearly) polarized photons, with the atomic quantization axis chosen along the photon propagation (polarization) direction, only the transition to the D-wave continuum will occur. The photoionization cross sections may then be obtained from Eq. (10) provided the D-wave contributions given in Tables III and IV are first multiplied by 1.8 and 0.9 for the circular and linear polarizations, respectively. It is apparent that measurements of the photoionization cross sections for unpolarized and for aligned P states of helium with circularly or linearly polarized light would lead to separate determinations of the individual S- and D-partial-wave contributions.

TABLE VI. The photoionization cross sections (in units of 10^{-18} cm^2) for unpolarized and aligned ($ML_0=1$) P states of helium evaluated using the length matrix elements. The numbers in parentheses are the powers of ten by which the entries are to be multiplied.

	Unpolarized He atoms		Polarized He atoms [a]	
k_1^2 (Ry)	$2\,^1P$	$2\,^3P$	$2\,^1P$	$2\,^3P$
0.15	2.983	3.952	3.258	4.300
0.20	1.983	3.183	2.178	3.461
0.25	1.406	2.376	1.550	2.587
0.30	1.024	1.825	1.134	1.991
0.40	5.743 (−1)	1.139	6.426 (−1)	1.247
0.60	2.116 (−1)	5.148 (−1)	2.426 (−1)	5.668 (−1)
0.80	9.057 (−2)	2.688 (−1)	1.070 (−1)	2.973 (−1)
1.00	4.288 (−2)	1.556 (−1)	5.269 (−2)	1.725 (−1)
1.20	2.204 (−2)	9.778 (−2)	2.854 (−2)	1.085 (−1)
1.40	1.235 (−2)	6.547 (−2)	1.708 (−2)	7.264 (−2)
1.60	8.103 (−3)	4.602 (−2)	1.194 (−2)	5.096 (−2)
1.80	7.194 (−3)	3.374 (−2)	1.074 (−2)	3.729 (−2)
2.00	9.735 (−3)	2.562 (−2)	1.374 (−2)	2.823 (−2)
2.20	2.061 (−2)	2.005 (−2)	2.695 (−2)	2.201 (−2)
2.40	1.589 (−1)	1.618 (−2)	2.190 (−1)	1.767 (−2)

[a] Unpolarized photons.

V. ASYMMETRY PARAMETERS

In the experimental investigation of photoionization from the P states of helium by photoelectron

TABLE VII. The photoelectron angular-distribution asymmetry parameter β for unpolarized $2\,^1P$ and $2\,^3P$ states of helium. The length and velocity results are denoted by L and V, respectively. The numbers in parentheses are the powers of ten by which the entries are to be multiplied.

	$2\,^1P$		$2\,^3P$	
k_1^2 (Ry)	β_L	β_V	β_L	β_V
0.15	1.566	1.538	1.696	
0.20	1.521	1.520	1.673	1.703
0.25	1.468	1.469	1.657	1.679
0.30	1.416	1.416	1.640	1.664
0.40	1.310	1.311	1.600	1.619
0.60	1.095	1.096	1.504	1.515
0.80	8.699 (−1)	8.701 (−1)	1.404	1.410
1.00	6.269 (−1)	6.170 (−1)	1.308	1.311
1.20	3.594 (−1)	3.266 (−1)	1.220	1.221
1.40	8.690 (−2)	4.163 (−2)	1.142	1.140
1.60	−7.228 (−2)	−5.417 (−2)	1.074	1.068
1.80	9.796 (−2)	2.243 (−1)	1.016	1.005
2.00	5.322 (−1)	6.514 (−1)	9.675 (−1)	9.504 (−1)
2.20	8.659 (−1)	9.220 (−1)	9.283 (−1)	9.058 (−1)
2.40	6.019 (−1)	6.260 (−1)	9.000 (−1)	8.727 (−1)

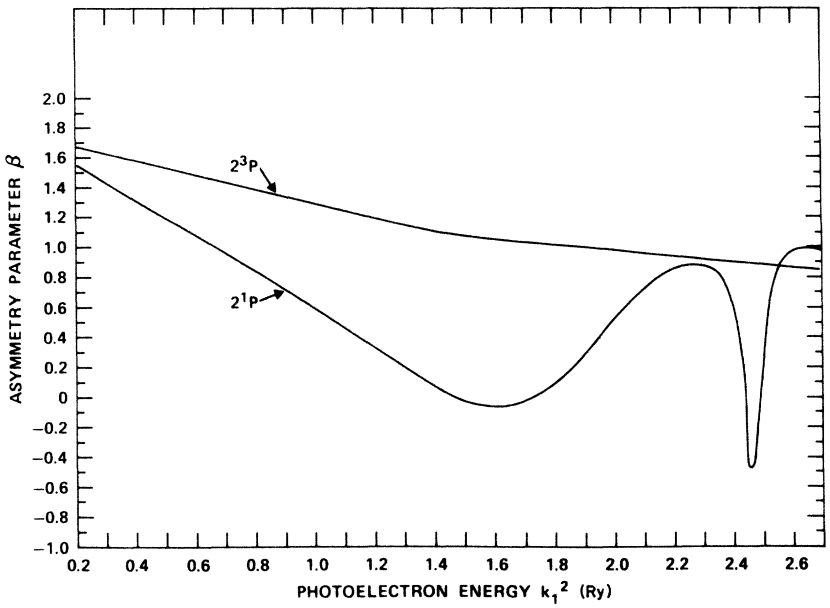

FIG. 4. The asymmetry parameter β for photoionization of unpolarized $2\,^1P$ and $2\,^3P$ states of helium, evaluated using the length matrix elements.

spectroscopy techniques which detect only the electrons ejected in a given direction, a knowledge of the asymmetry parameters would be required in order to relate the observed electron intensity to the total cross sections. The calculated values of the asymmetry parameter β for unpolarized $2\,^1P$ and $2\,^3P$ states of helium are presented in Table VII for the photoelectron energy range $0.15 \leq k_1^2 \leq 2.4$ and are shown over a more extended energy range in Fig. 4. The asymmetry parameters β_2 and β_4 for photoionization of aligned $2\,^1P$ and $2\,^3P$ states of helium by unpolarized light are shown in Fig. 5.

For ionization of aligned P states by right circularly polarized photons the energy-independent values of the asymmetry parameters are found to be $\beta_2 = -1.429$ and $\beta_4 = 0.4286$, while in the case of linearly polarized light the values are $\beta_2 = 0.7143$ and $\beta_4 = -1.714$.

The most striking features occur in the $2\,^1P$ case, where the lowest ^1S and ^1D helium resonances produce conspicuous energy variations in the asymmetry parameters. For an understanding of the behavior of the $2\,^1P$ asymmetry parameter β illustrated in Fig. 4, it may be noted

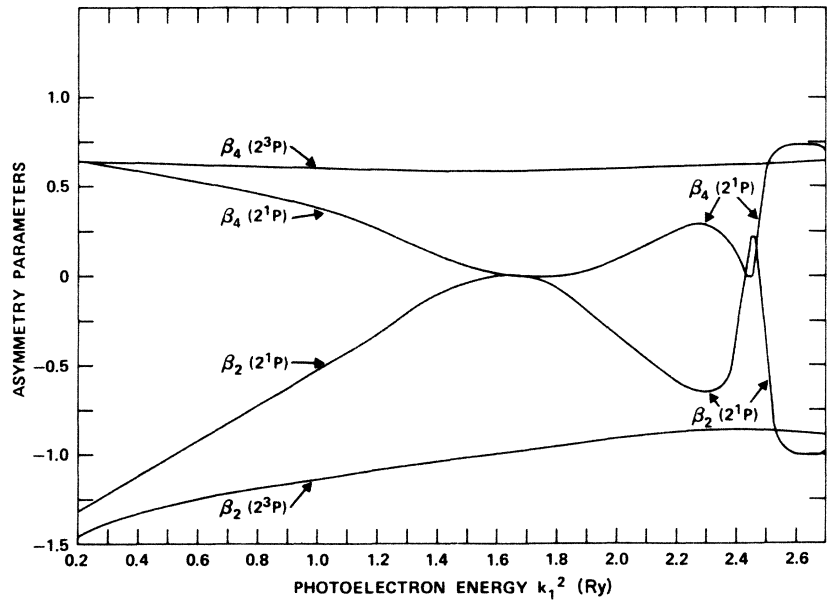

FIG. 5. The asymmetry parameters β_2 and β_4 for photoionization of aligned $2\,^1P$ and $2\,^3P$ states of helium by unpolarized light, evaluated using the length matrix elements.

that the hypothetical values of β associated with pure S and D transitions are 0 and 1, respectively.

VI. CONCLUSIONS

The photoionization cross sections presented in this paper should be accurate to within 10% or better. The introduction of Hylleraas terms into the final-state continuum wave functions would lead to greater precision and a more balanced calculation.

Taking into consideration the available experimental techniques, it appears desirable to attempt a measurement of the $2\,^1P$ helium photoionization cross section by excitation of a helium gas with $2\,^1P$—$1\,^1S$ resonance radiation from a helium discharge and subsequent ionization using a tunable laser.

ACKNOWLEDGMENTS

I wish to acknowledge Professor P. G. Burke's important contribution to the present calculations, which could not have been performed without the use of his collision code. I would also like to thank R. Baxter, J. Bredekamp, and E. Sullivan for their generous assistance in setting up the computer programs at the Goddard Space Flight Center.

---

*National Academy of Sciences—National Research Council Resident Research Associate.

[1]H. R. Griem, *Plasma Spectroscopy* (McGraw-Hill, New York, 1964).
[2]V. P. Myerscough and G. Peach, *Case Studies in Atomic Collision Physics, II* (North-Holland, Amsterdam, 1972).
[3]J. Bakos, A. Kiss, L. Szabo, and M. Tendler, Phys. Lett. A39, 317 (1972).
[4]R. F. Stebbings, F. B. Dunning, F. K. Tittel, and R. D. Rundel, Phys. Rev. Lett. 30, 815 (1973).
[5]V. L. Jacobs, Phys. Rev. A 3, 289 (1971).
[6]V. L. Jacobs, Phys. Rev. A 4, 939 (1972).
[7]V. L. Jacobs and P. G. Burke, J. Phys. B 5, L67 (1972).
[8]V. L. Jacobs and P. G. Burke, J. Phys. B 5, 2272 (1972).
[9]H. A. Hyman, V. L. Jacobs, and P. G. Burke, J. Phys. B 5, 2282 (1972).
[10]M. O. Krause and F. Wuilleumier, J. Phys. B 5, L143 (1972).
[11]P. G. Burke and D. D. McVicar, Proc. Phys. Soc., Lond. 80, 616 (1962).
[12]D. W. Norcross, J. Phys. B 4, 652 (1971).
[13]L. Goldberg, Astrophys. J. 90, 414 (1939).
[14]A. Burgess and M. J. Seaton, Mon. Not. R. Astron. Soc. 120, 121 (1960).
[15]A. Anderson and H. R. Griem, *Ionization Phenomena in Gases* (North-Holland, Amsterdam, 1963), Vol. 3, p. 293.
[16]H. A. Bethe and E. E. Salpeter, *Quantum Mechanics of One- and Two-Electron Atoms* (Academic, New York, 1957).
[17]J. Cooper and R. N. Zare, J. Chem. Phys. 48, 942 (1968).
[18]U. Fano and D. Dill, Phys. Rev. A 6, 185 (1972).
[19]V. L. Jacobs, J. Phys. B 5, 2257 (1972).
[20]U. Fano and G. Racah, *Irreducible Tensorial Sets* (Academic, New York, 1959).
[21]Y. Accad, C. L. Pekeris, and B. Schiff, Phys. Rev. A 4, 516 (1971).
[22]P. G. Burke, *The Physics of Electronic and Atomic Collisions* (JILA, Boulder, Colo., 1968).
[23]U. Fano. Phys. Rev. 124, 1866 (1961).